

Supporting Information

Cation Optimization for Bifacial Surface Passivation in Efficient and Stable Perovskite Solar Cells

Jie Zhao^{†ab}, *Nitish Rai*^{†ab}, *Juan F. Benitez-Rodriguez*^c, *Wenqi Yan*^{ab}, *Luke J. Sutherland*^{cd},
Junlin Yan^c, *Anthony S. R. Chesman*^d, *Jacek Jasieniak*^{ac}, *Jianfeng Lu*^e, *Udo Bach*^{*ab}

^a *ARC Center of Excellence in Exciton Science, Monash University, Victoria 3800, Australia*

^b *Department of Chemical and Biological Engineering, Monash University, Victoria 3800, Australia*

^c *Department of Materials Science and Engineering, Monash University, Victoria 3800, Australia*

^d *CSIRO Manufacturing, Clayton, Victoria 3168, Australia*

^e *State Key Laboratory of Silicate Materials for Architectures, Wuhan University of Technology, Wuhan 430070, China*

[†] *These authors contributed equally to this work.*

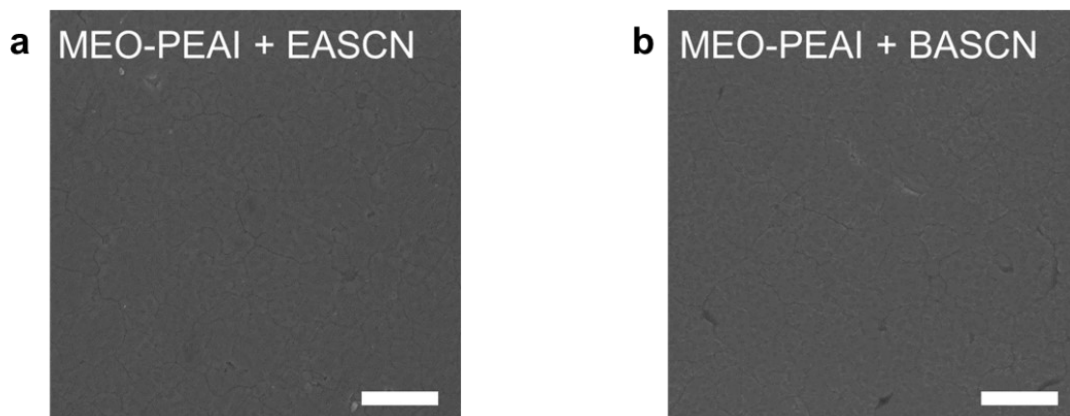


Figure S1. a, b, Scanning electron microscopy (SEM) images of buried interface of MEO-PEAI + EASCN and MEO-PEAI + BASCN treated perovskite films. Scale bars, 1 μ m.

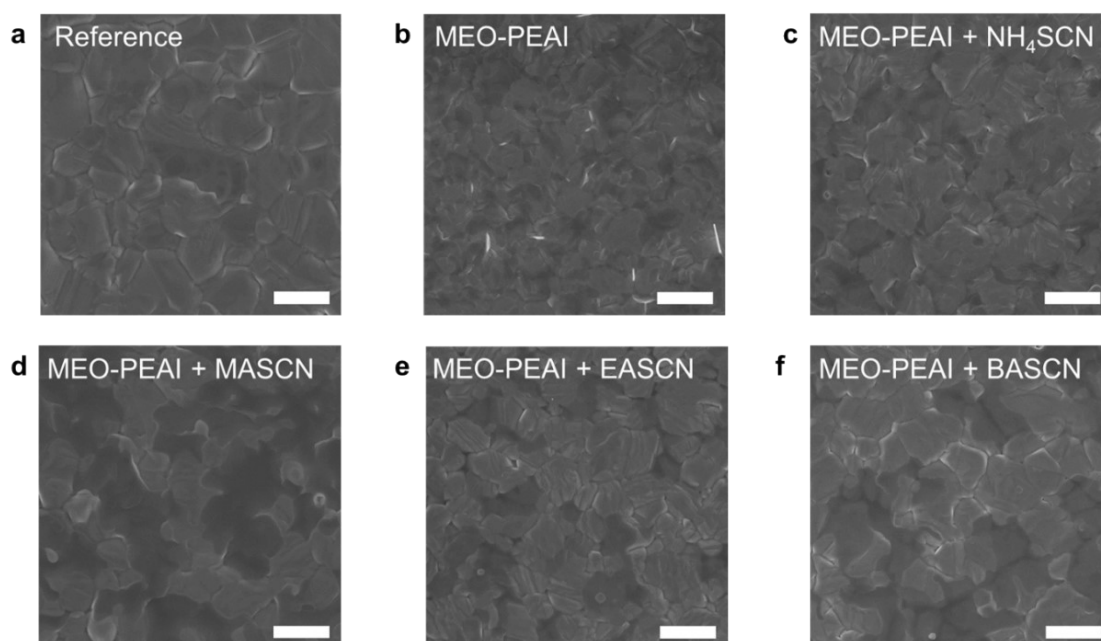


Figure S2. (a-f), Scanning electron microscopy (SEM) images of top surface of the reference, MEO-PEAI, MEO-PEAI + NH₄SCN, MEO-PEAI + MASCN, MEO-PEAI + EASCN and MEO-PEAI +BASCN treated perovskite films. Scale bars, 1 μ m.

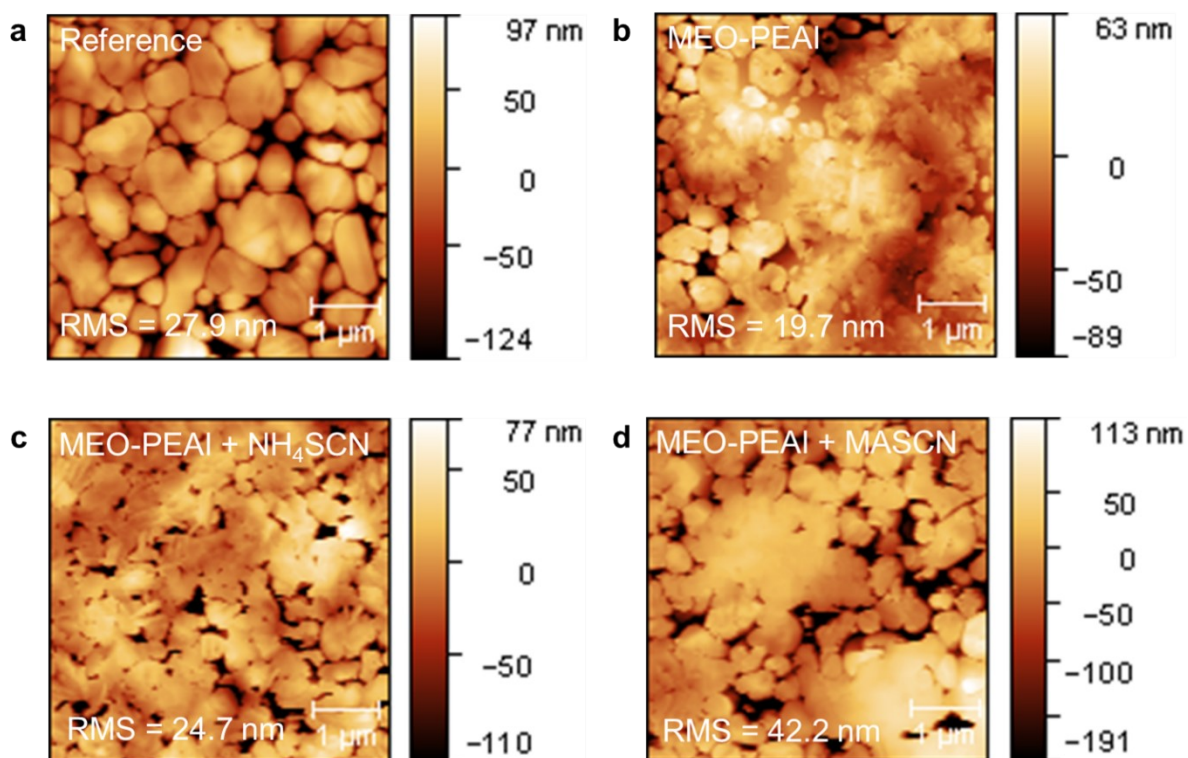


Figure S3. (a-d), Atomic force microscopy (AFM) images of exposed surface of the reference, MEO-PEAI, MEO-PEAI + NH_4SCN and MEO-PEAI + MASCN treated perovskite films.

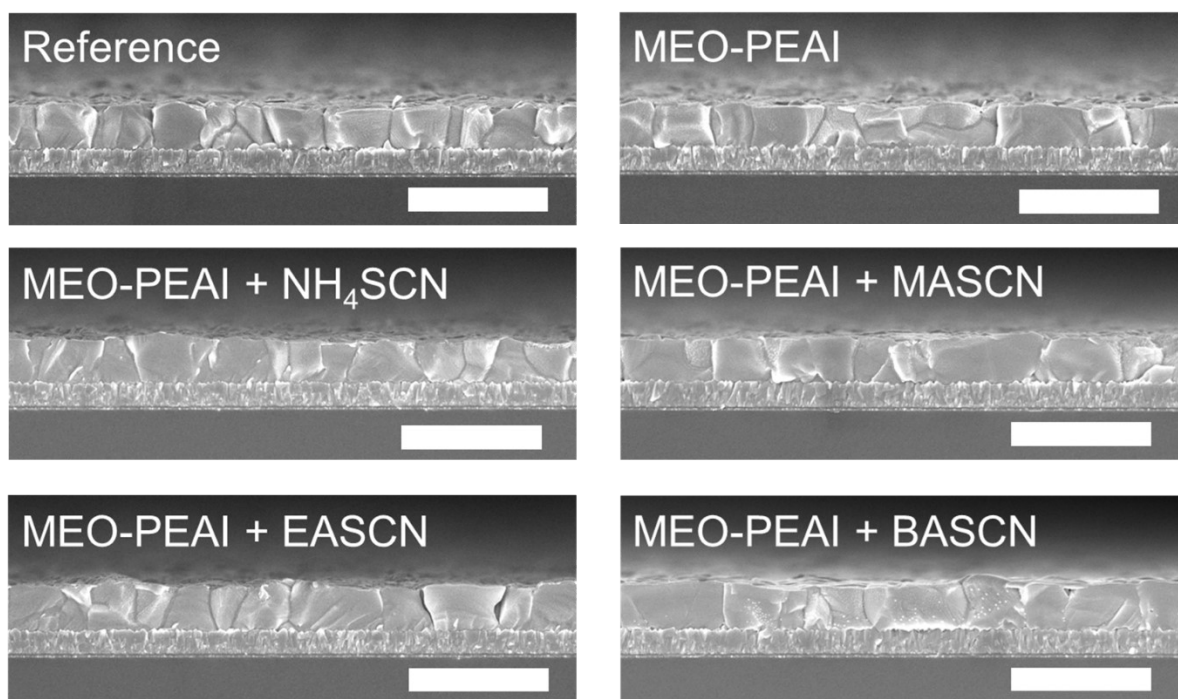


Figure S4. Cross sectional SEM images of perovskite films. (Scale bar: $2\mu\text{m}$)

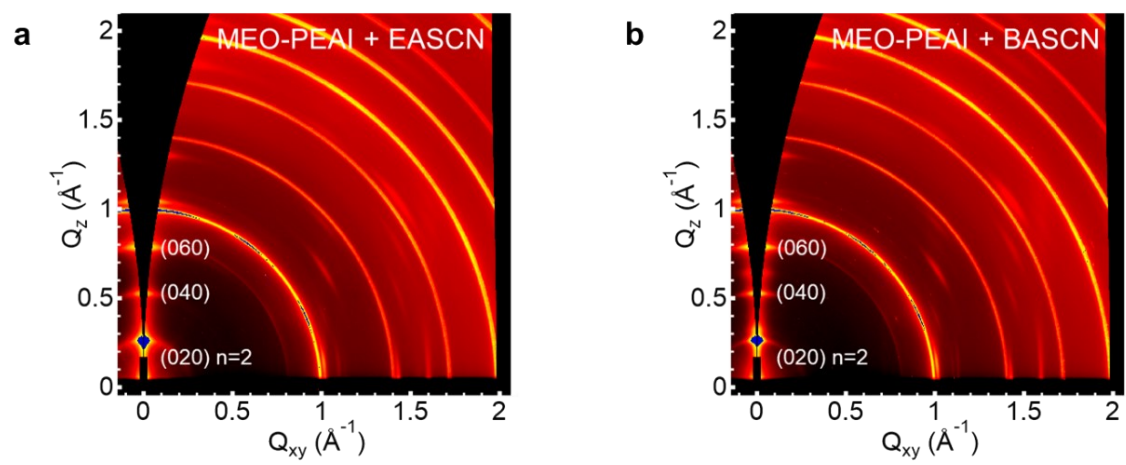
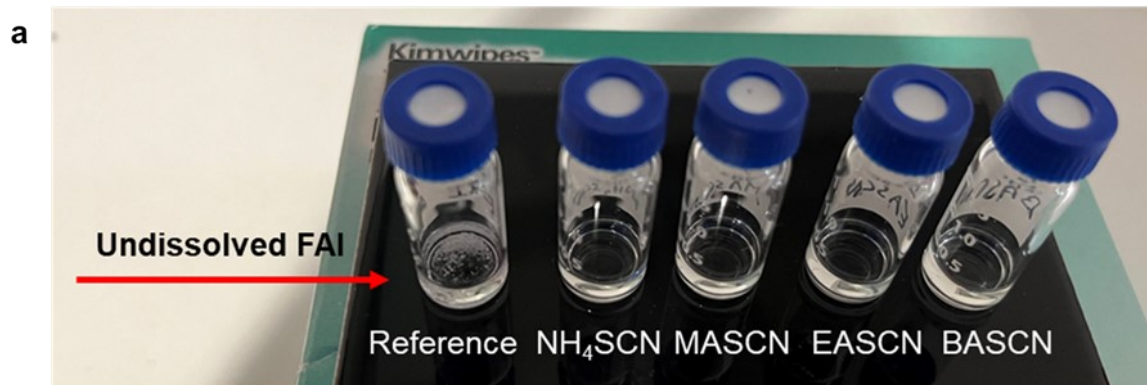
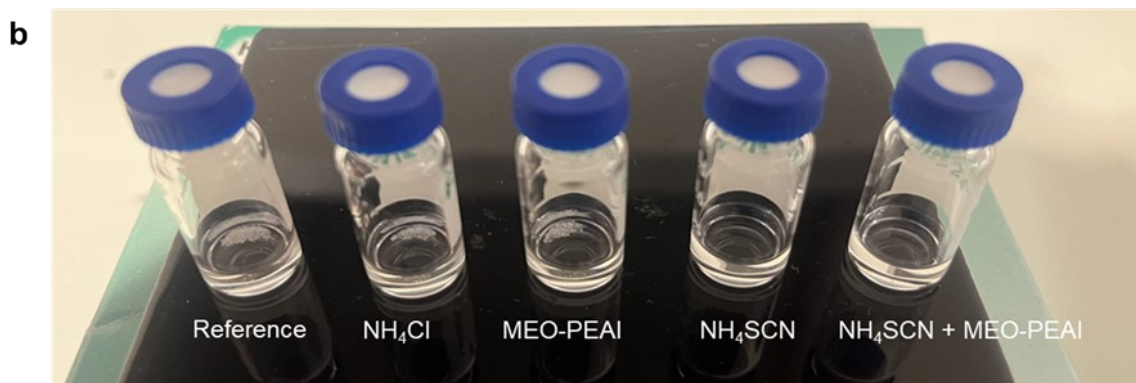


Figure S5. a, b, GIWAXS patterns of MEO-PEAI + EASCN and MEO-PEAI + BASCN treated perovskite films.



1.31M FAI + 10 mg/mL of different thiocyanate salt in 2-propanol



20 mg/mL FAPbI_3 vs 20 mg/mL $\text{FAPbI}_3 + 10\text{mg/mL}$ NH_4SCN in IPA

Figure S6. (a-c), Solubility limit photo of FAI and FAPbI_3 in 2-propanol (IPA).

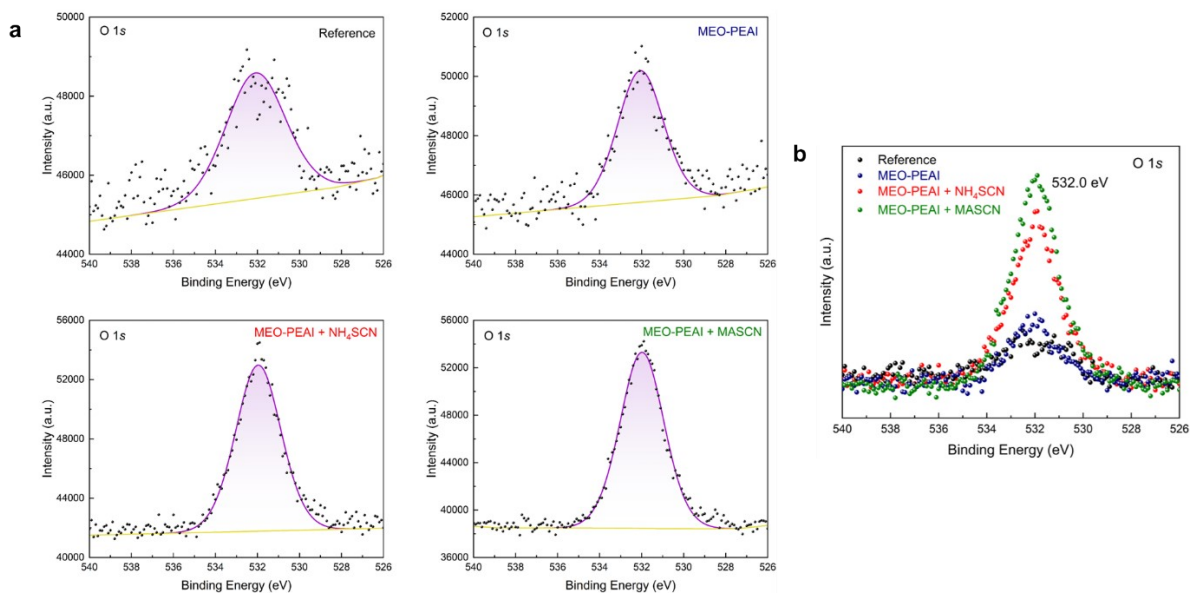


Figure S7. a, X-ray photoelectron spectroscopy (XPS) measurements of oxygen at the buried interface obtained by peeling off the perovskite films. b, Summary of XPS spectra of oxygen for perovskite films. (Graphs are offset for clarity.)

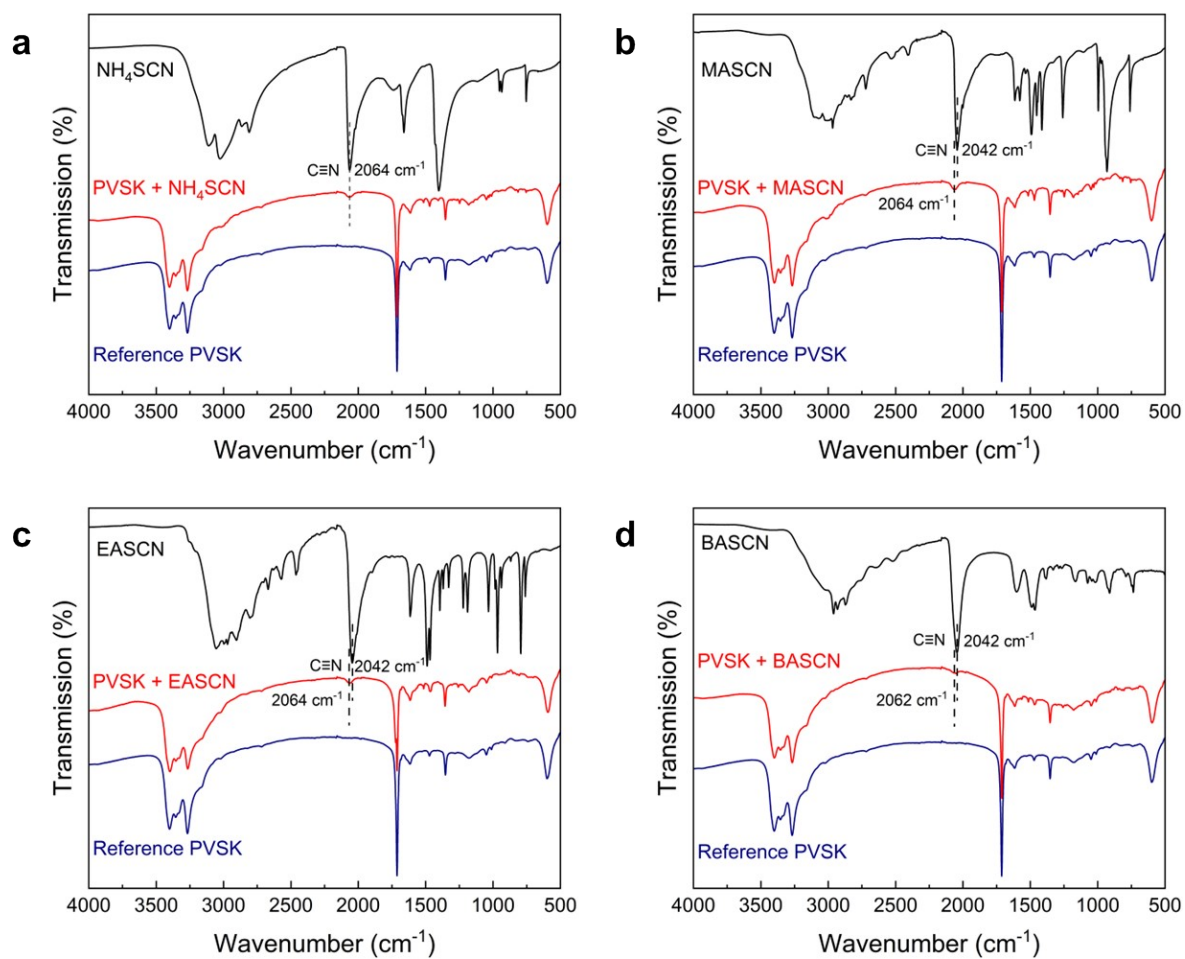


Figure S8. FTIR spectra of perovskite samples treated with (a-d) NH₄SCN, MASCN, EASCN and BASCN. (Graphs are offset for clarity)

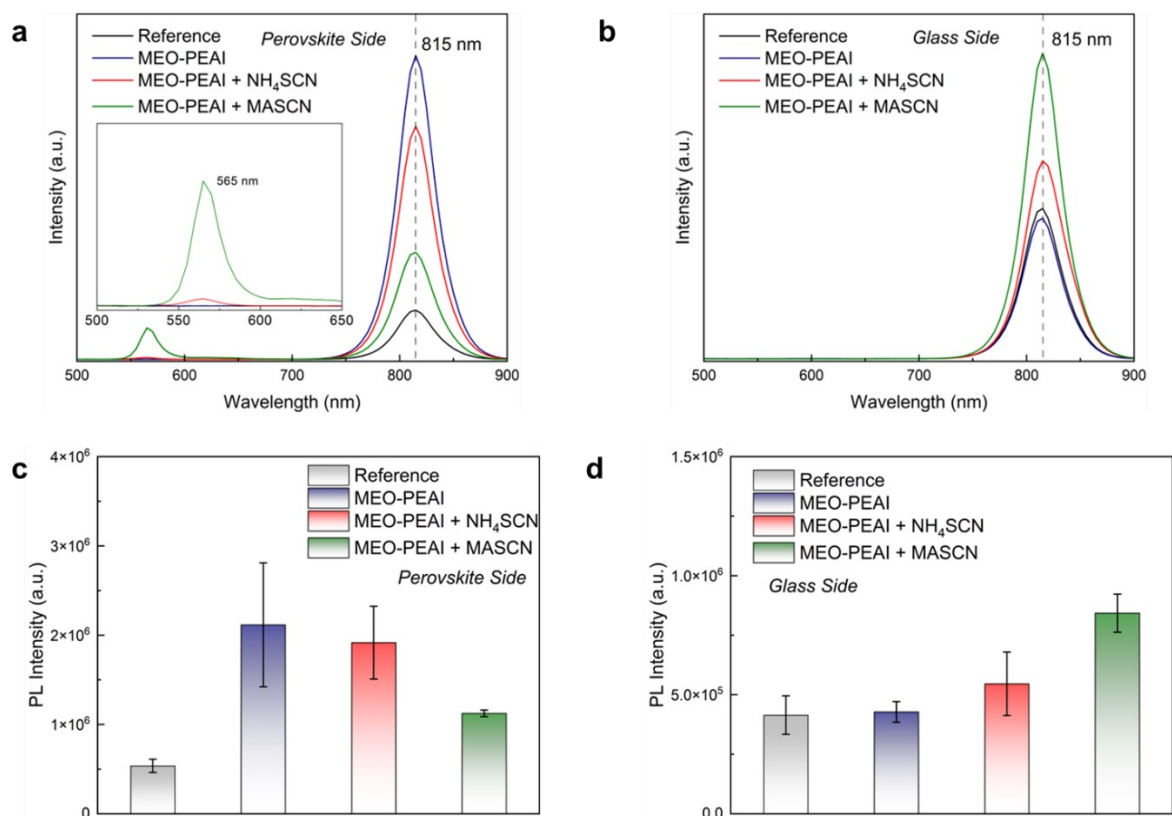


Figure S9. a, b, Champion steady-state photoluminescence (PL) spectra of perovskite films excited from a) the perovskite side and b) the glass side. c, d, Statistical data of PL peak intensity excited from c) the perovskite side and d) the glass side. Measurements were conducted on two samples with two spots per sample to account for variations in PL intensity across different sample positions and between samples.

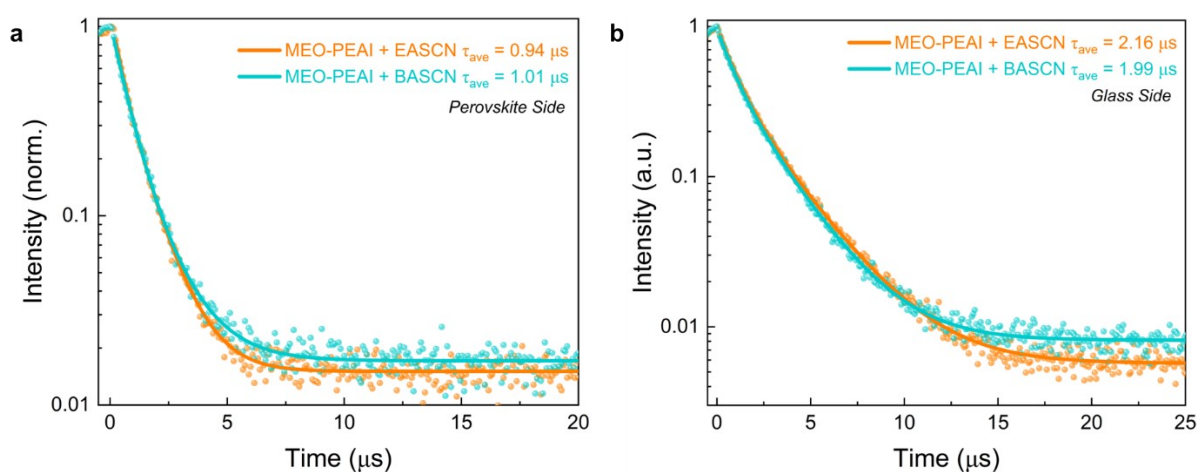


Figure S10. a, b, Time-resolved photoluminescence (TRPL) of MEO-PEAI + EASCN and MEO-PEAI + BASCN treated perovskite films excited from a) the perovskite side and b) the glass side.

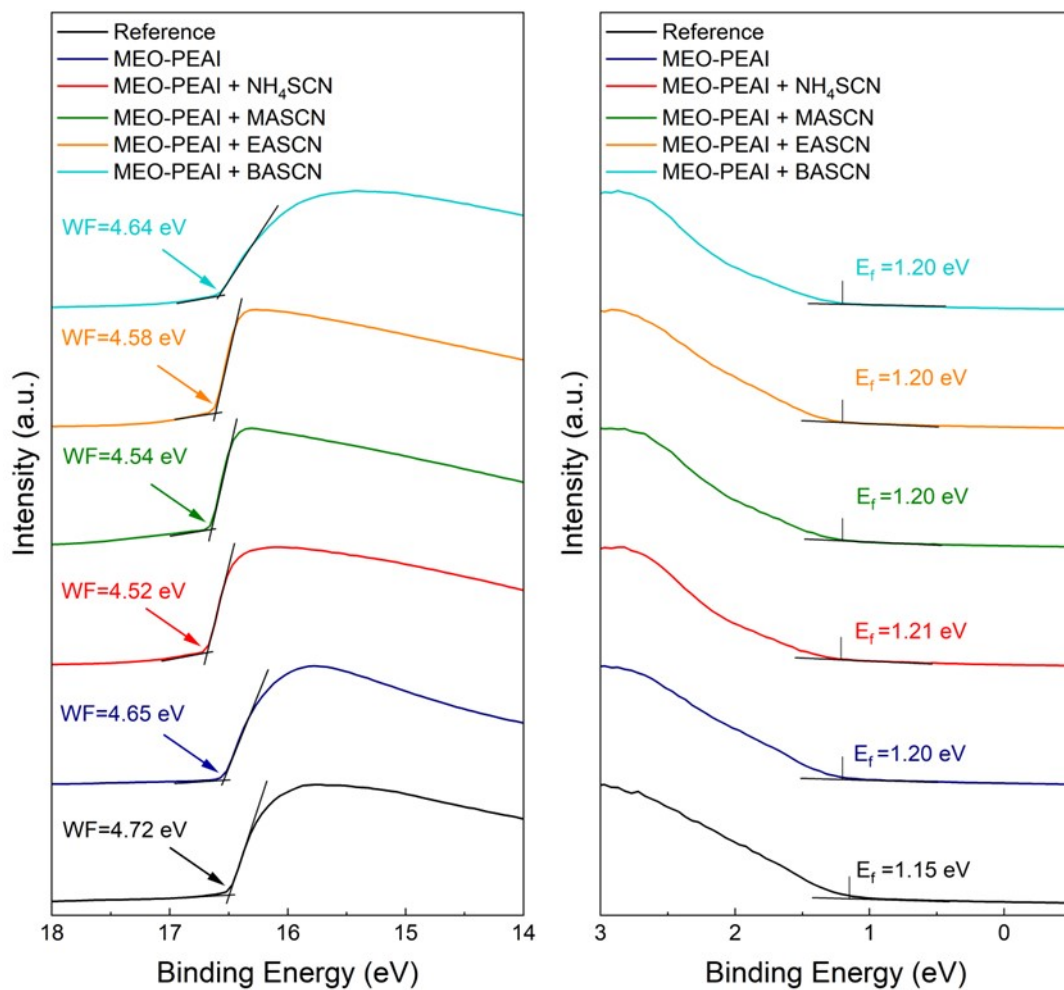


Figure S11. Cut-off region of UPS of different perovskite films.

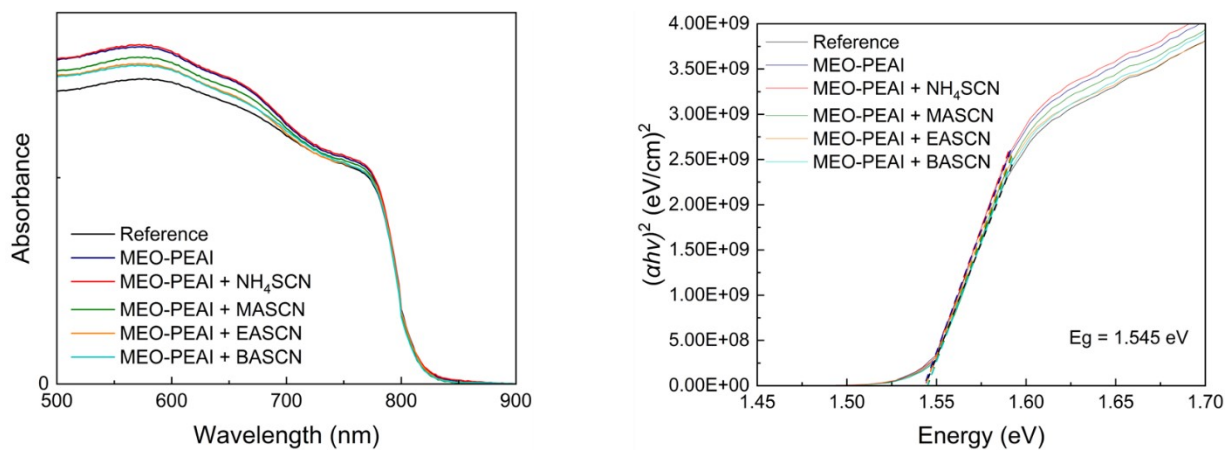


Figure S12. UV-vis spectra and Tauc plot of perovskite thin films.

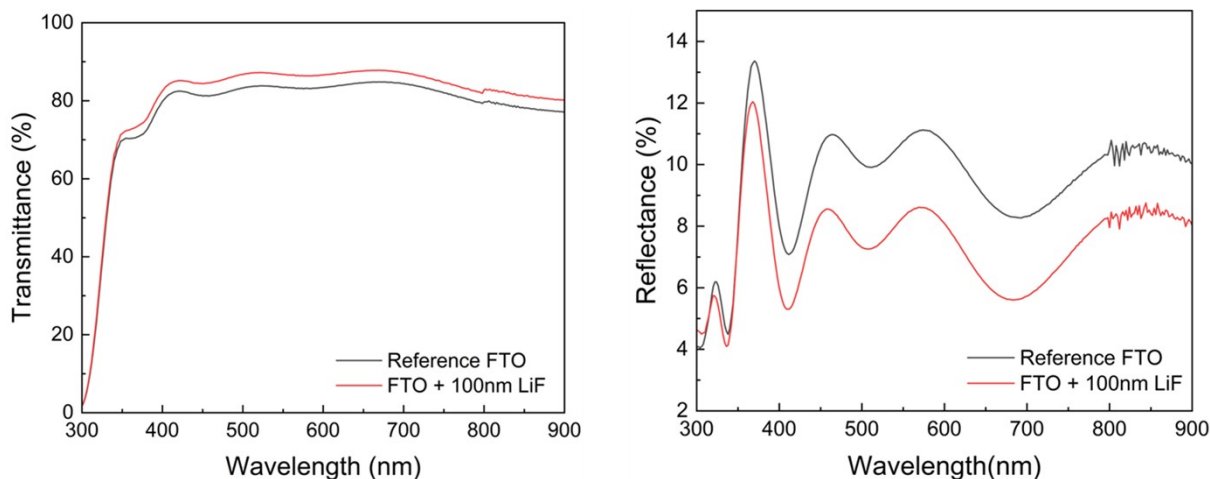


Figure S13. (Left) Transmittance and (right) reflectance of FTO-coated glass and FTO-coated glass treated with a 100 nm LiF anti-reflective layer.

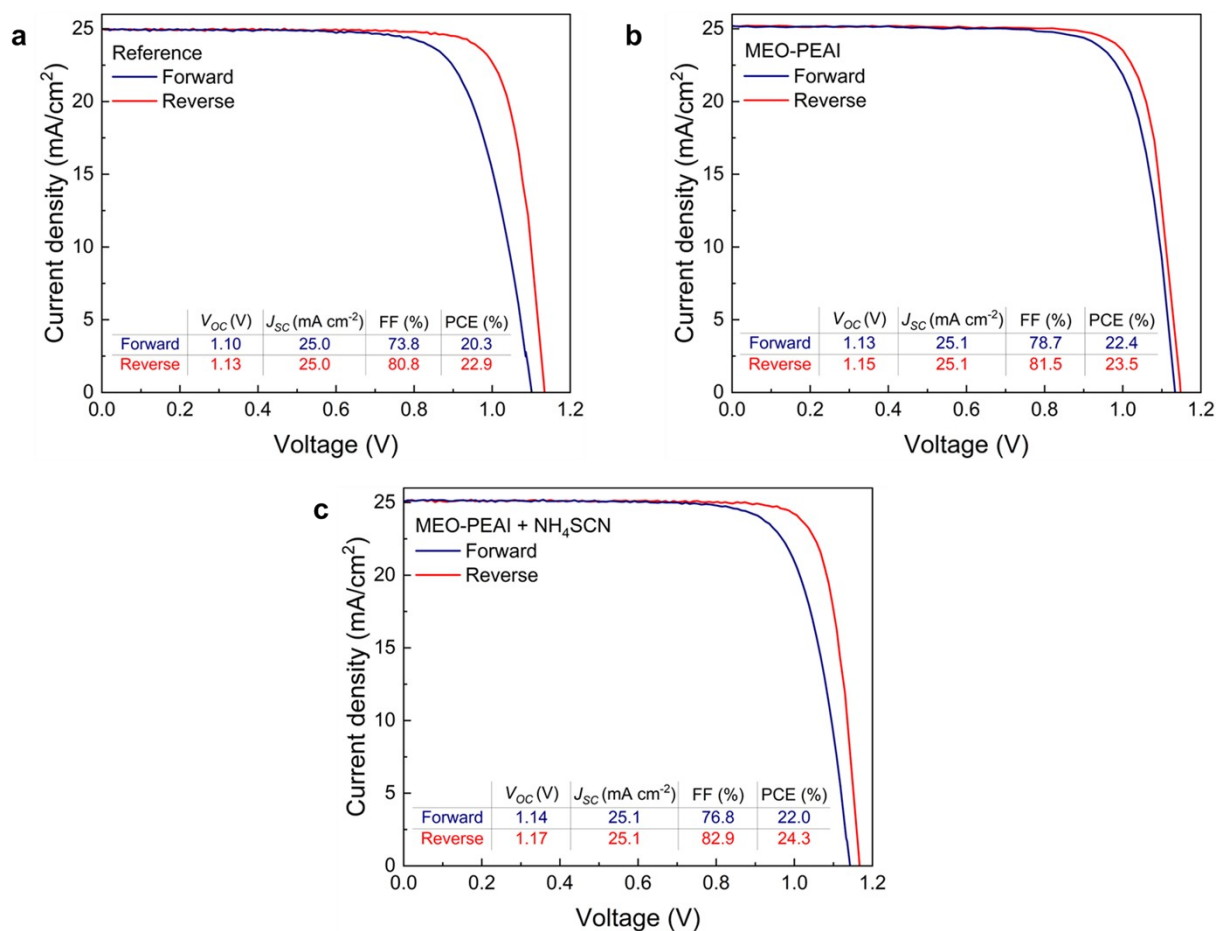


Figure S14. J - V characteristics of champion reference (a), MEO-PEAI treated (b) device and MEO-PEAI + NH_4SCN treated (c) device in both scan direction (mask area: 0.09 cm²).

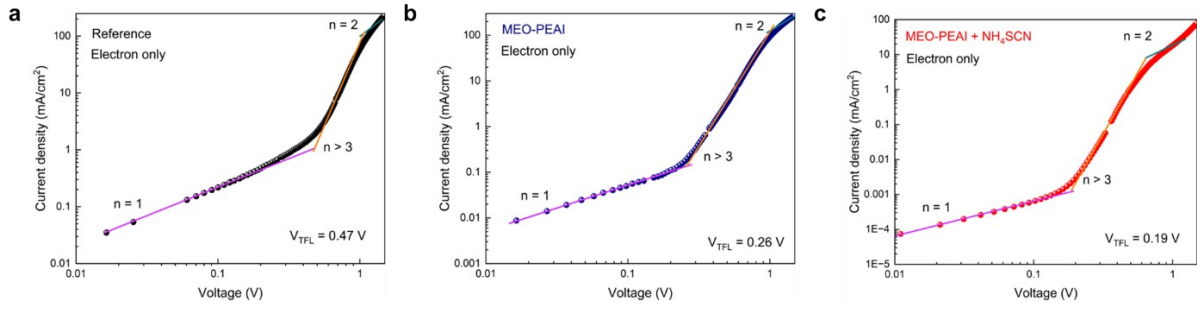


Figure S15. The space charge limited current (SCLC) curves for the electron-only devices (a) reference ($N_{trap} = 4.44 \times 10^{15} \text{ cm}^{-3}$) and treated with (b) MEO-PEAI ($N_{trap} = 2.46 \times 10^{15} \text{ cm}^{-3}$) and (c) MEO-PEAI + NH_4SCN ($N_{trap} = 1.8 \times 10^{15} \text{ cm}^{-3}$). The device architecture was $\text{FTO}|\text{SnO}_2|(\text{FAPbI}_3)_{0.99}(\text{MAPbBr}_3)_{0.01}|\text{Passivation layer}|\text{PCBM}|\text{Au}$.

The trap density (N_{trap}) was calculated according to the following formula:

$$N_{trap} = 2\varepsilon_0\varepsilon_r V_{TFL}/eL^2$$

Where $\varepsilon_0 = 8.85 \times 10^{-12} \text{ F m}^{-1}$ and $\varepsilon_r = 30.8$ are the vacuum permittivity and the relative dielectric constants of $(\text{FAPbI}_3)_{0.99}(\text{MAPbBr}_3)_{0.01}$, respectively; e is the elementary charge of the electron; $L \approx 600 \text{ nm}$ is the thickness of the perovskite film measured by the cross-sectional SEM.

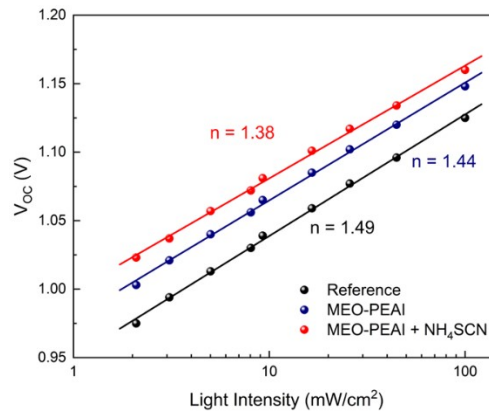


Figure S16. Light intensity dependence of V_{OC} with corresponding slopes by linear fitting.

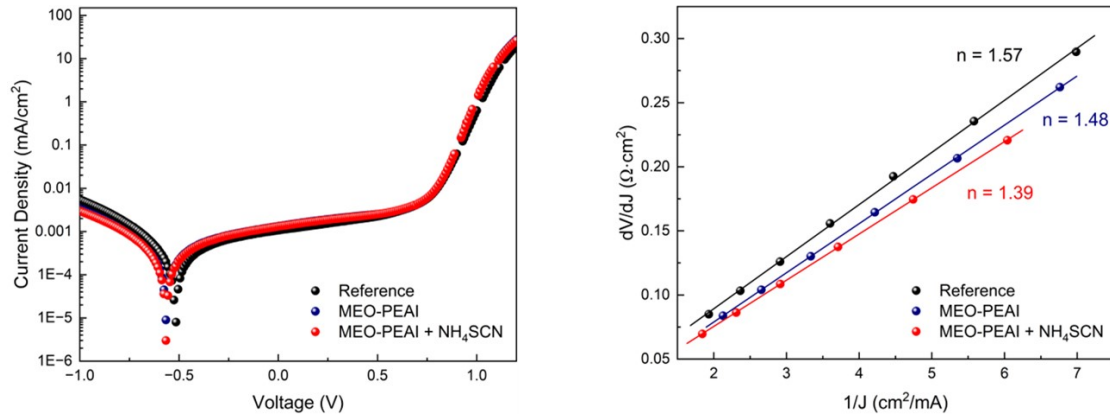


Figure S17. Dark J - V characteristics and dark J - V scan analysis: dV/dJ vs. J^{-1} plot with corresponding slopes by linear fitting to indicate the ideality factor.

Table S1. TRPL fitting parameters.

Sample (Perovskite side)	A_1	τ_1 (ns)	A_2 (ns)	τ_2	$\langle\tau\rangle$ (ns)
Reference	2.26	2394	4.27	875	1772
MEO-PEAI	3.80	2735	7.35	920	2020
MEO-PEAI + NH ₄ SCN	4.16	3705	7.85	1110	2767
MEO-PEAI + MASCN	2.38	1859	1.72	617	1618
MEO-PEAI + EASCN	1.66	1091	1.25	458	940
MEO-PEAI + BASCN	0.75	1434	1.9	647	1013
Sample (Glass side)	A_1	τ_1 (ns)	A_2 (ns)	τ_2	$\langle\tau\rangle$ (ns)
Reference	2.11	1732	2.42	619	1410
MEO-PEAI	2.71	1979	2.65	728	1648
MEO-PEAI + NH ₄ SCN	4.94	2808	5.76	932	2285
MEO-PEAI + MASCN	3.49	4217	8.19	1353	2986
MEO-PEAI + EASCN	3.77	2604	3.93	881	2155
MEO-PEAI + BASCN	2.93	2329	2.43	838	1986

Table S2. Work function and valence band values derived from UPS.

Sample	Work Function (eV)	Valence Band (eV)
Reference	4.72	-5.87
MEO-PEAI	4.65	-5.85
MEO-PEAI + NH ₄ SCN	4.52	-5.73
MEO-PEAI + MASCN	4.54	-5.74
MEO-PEAI + EASCN	4.58	-5.78
MEO-PEAI + BASCN	4.64	-5.94